Supporting information

Nature-inspired compositional control of transition-metal-doped ammoniotinsleyite and spheniscidite particles for the design of color hue

Hiroaki Uchiyama*, Daisuke Nagoshi and Yuki Nagasu

Corresponding Author

Hiroaki Uchiyama, Department of Chemistry and Materials Engineering, Kansai University, 3-3-35 Yamate-cho, Suita, 564-8680, Japan. E-mail: h_uchi@kansai-u.ac.jp (H. Uchiyama)

Authors

Daisuke Nagoshi and Yuki Nagasu, Department of Chemistry and Materials Engineering, Kansai University, 3-3-35 Yamate-cho, Suita, 564-8680, Japan

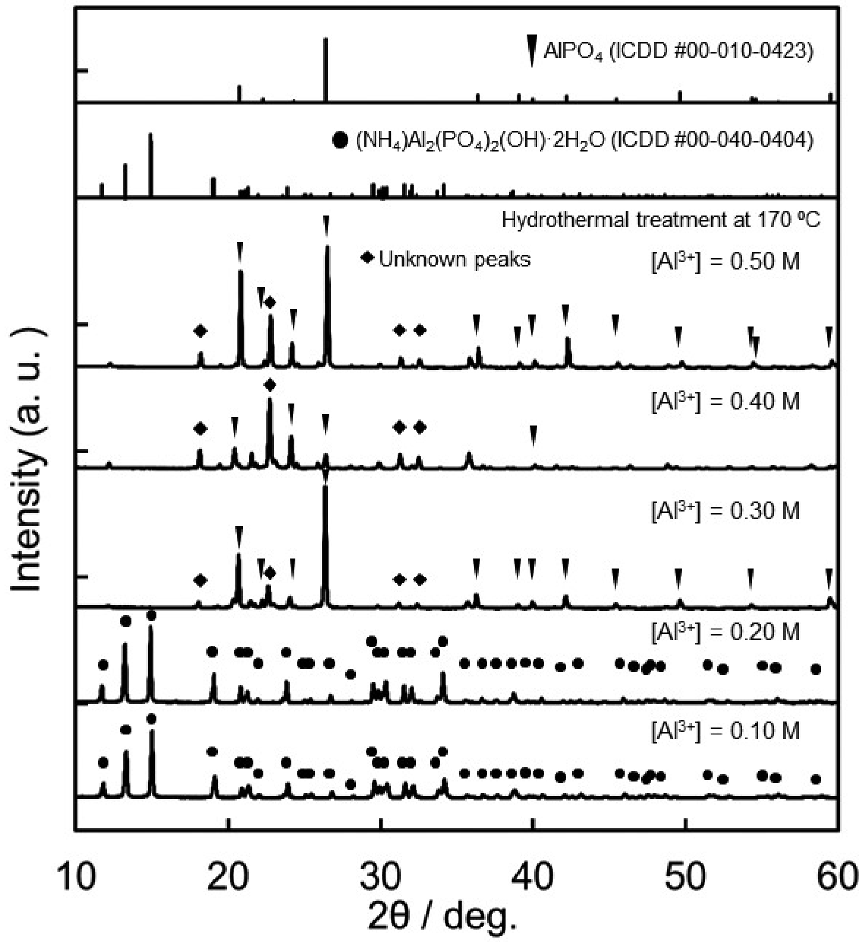

Fig. S1 XRD patterns of the aluminum phosphate precipitates obtained at $[AlCl_3]$ = 0.10–0.50 M by hydrothermal treatment at 170 °C.

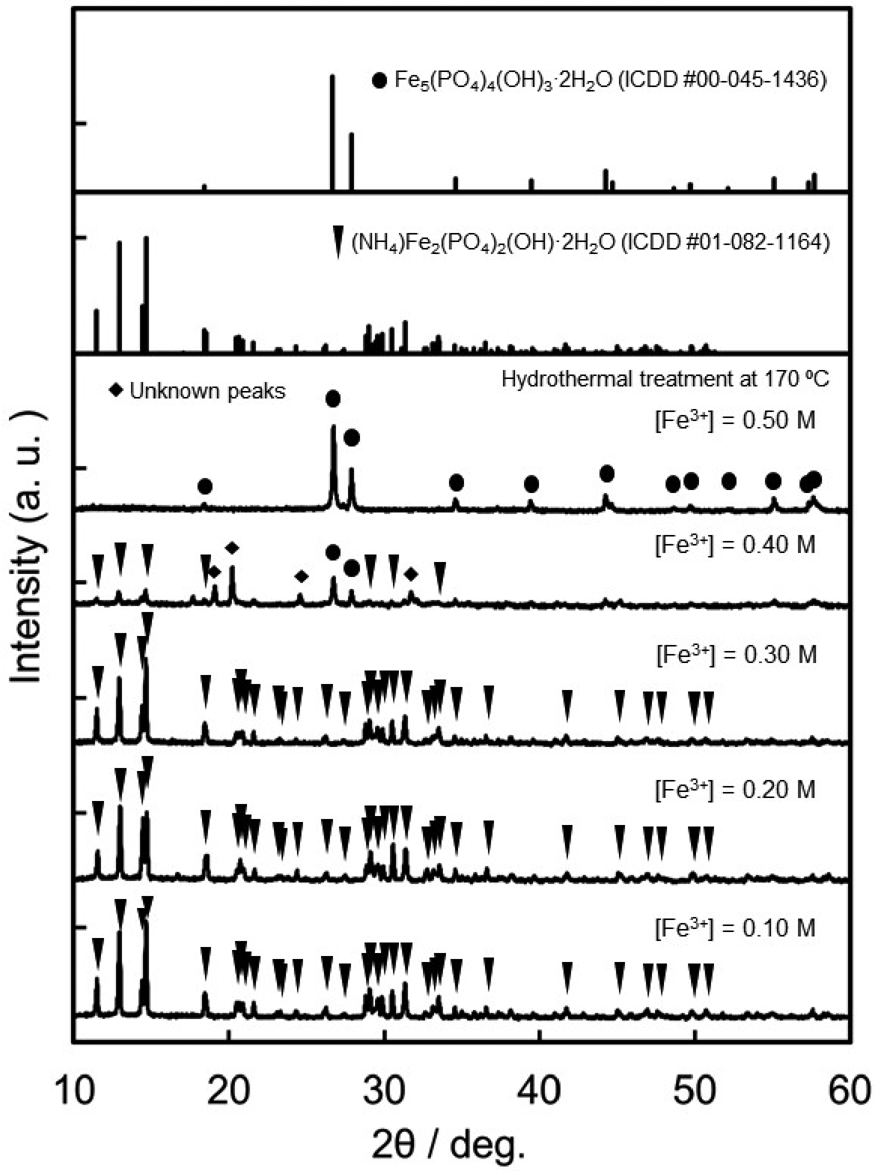

Fig. S2 XRD patterns of the iron phosphate precipitates obtained at $[FeCl_3 \cdot 6H_2O]$ = 0.10–0.50 M by hydrothermal treatment at 170 °C.

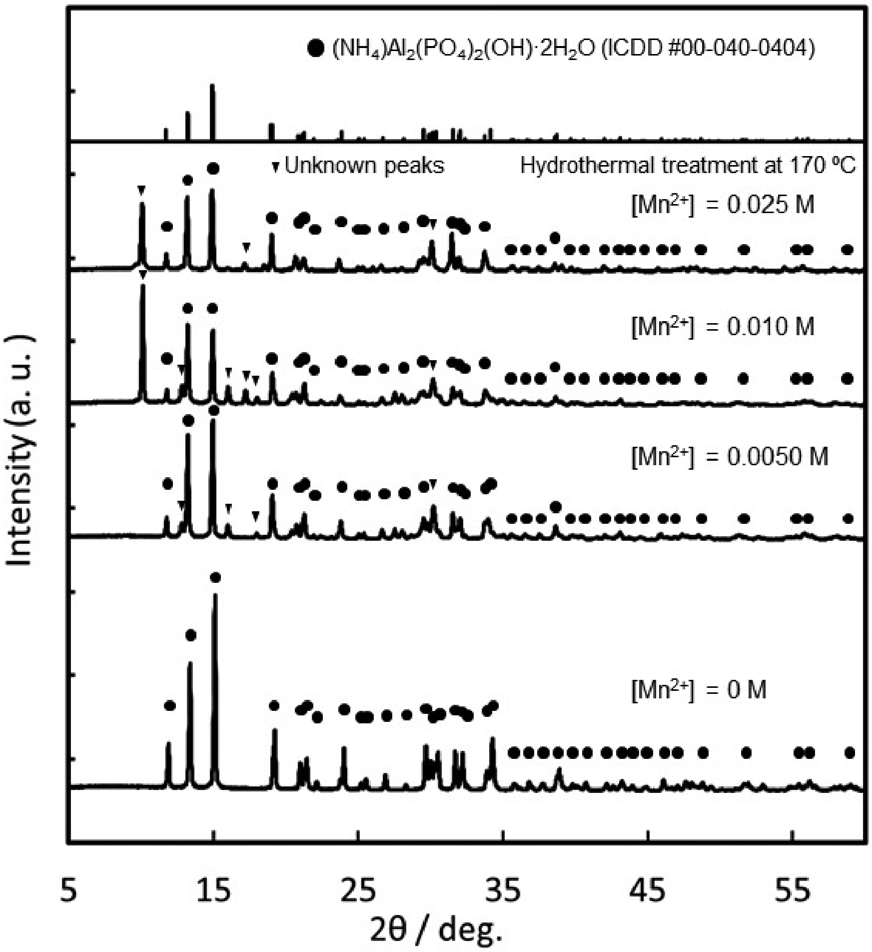

Fig. S3 XRD patterns of the Mn^{2+}-doped aluminum phosphate precipitates obtained at $[AlCl_3]$ = 0.10 M and $[MnCl_2{\cdot}4H_2O]$ = 0–0.025 M by hydrothermal treatment at 170 °C.

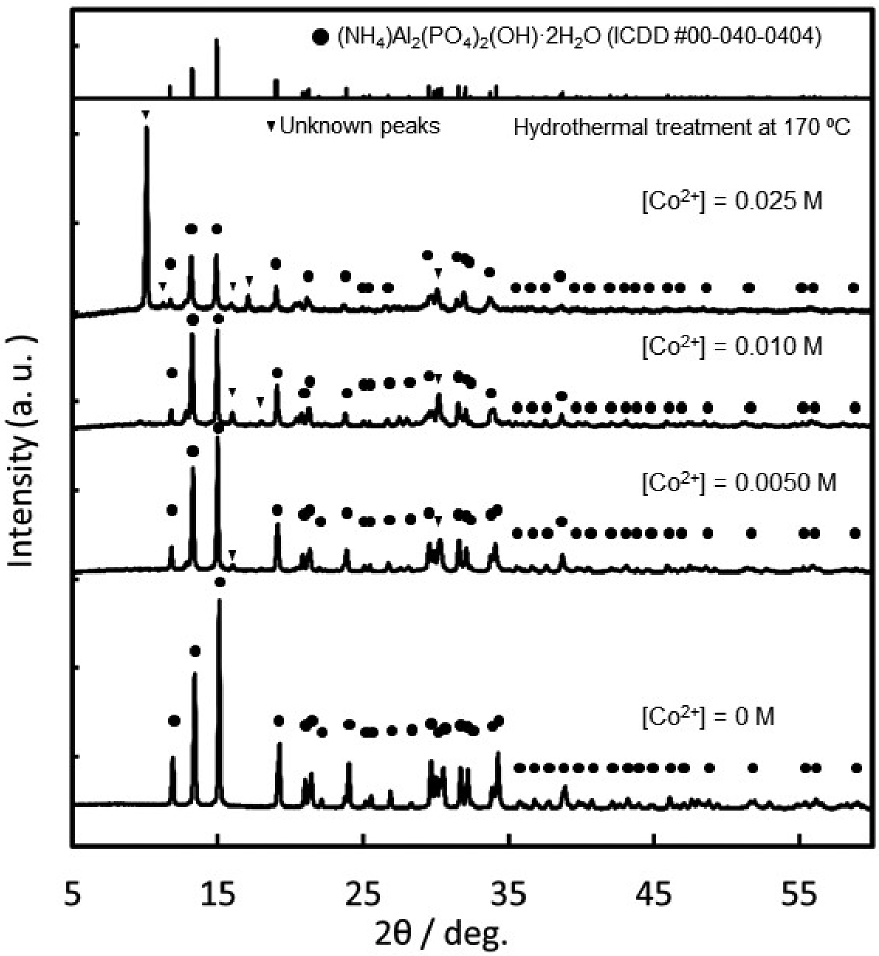

Fig. S4 XRD patterns of the Co^{2+}-doped aluminum phosphate precipitates obtained at [$AlCl_3$] = 0.10 M and [$CoCl_2 \cdot 6H_2O$] = 0–0.025 M by hydrothermal treatment at 170 °C.

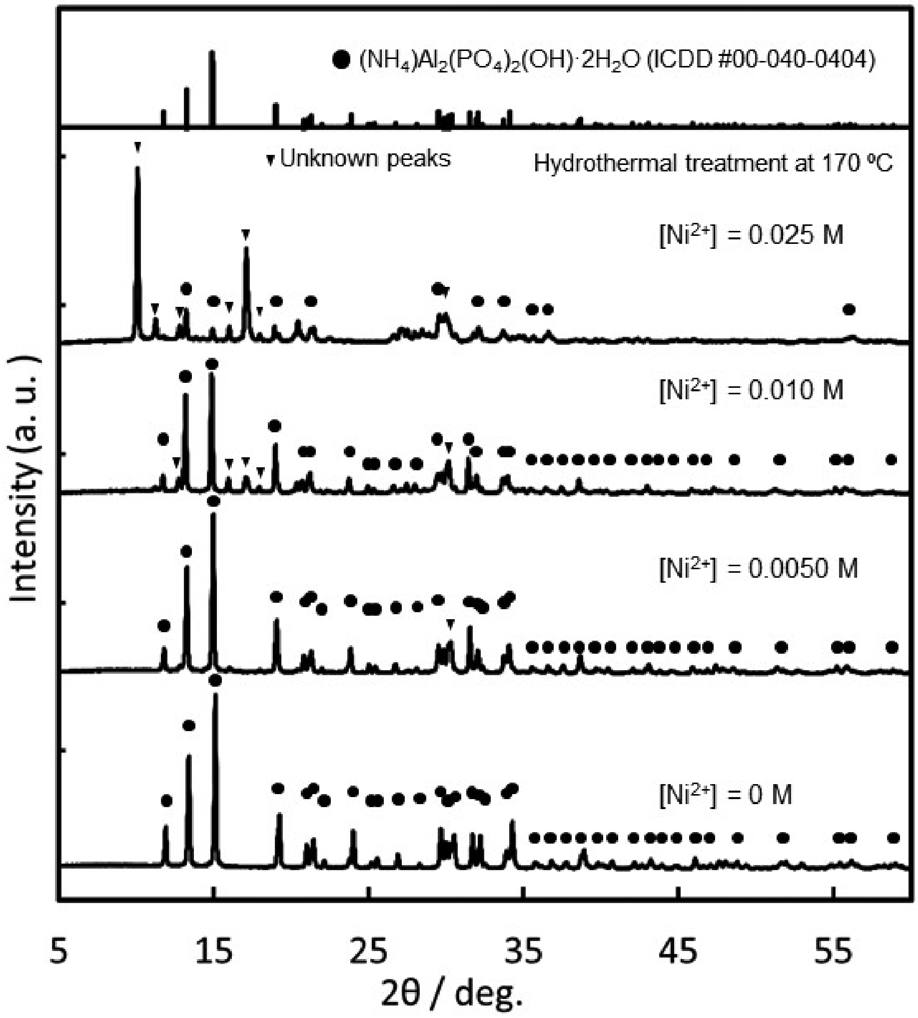

Fig. S5 XRD patterns of the Ni^{2+}-doped aluminum phosphate precipitates obtained at $[AlCl_3]$ = 0.10 M and $[NiCl_2\cdot 6H_2O]$ = 0–0.025 M by hydrothermal treatment at 170 °C.

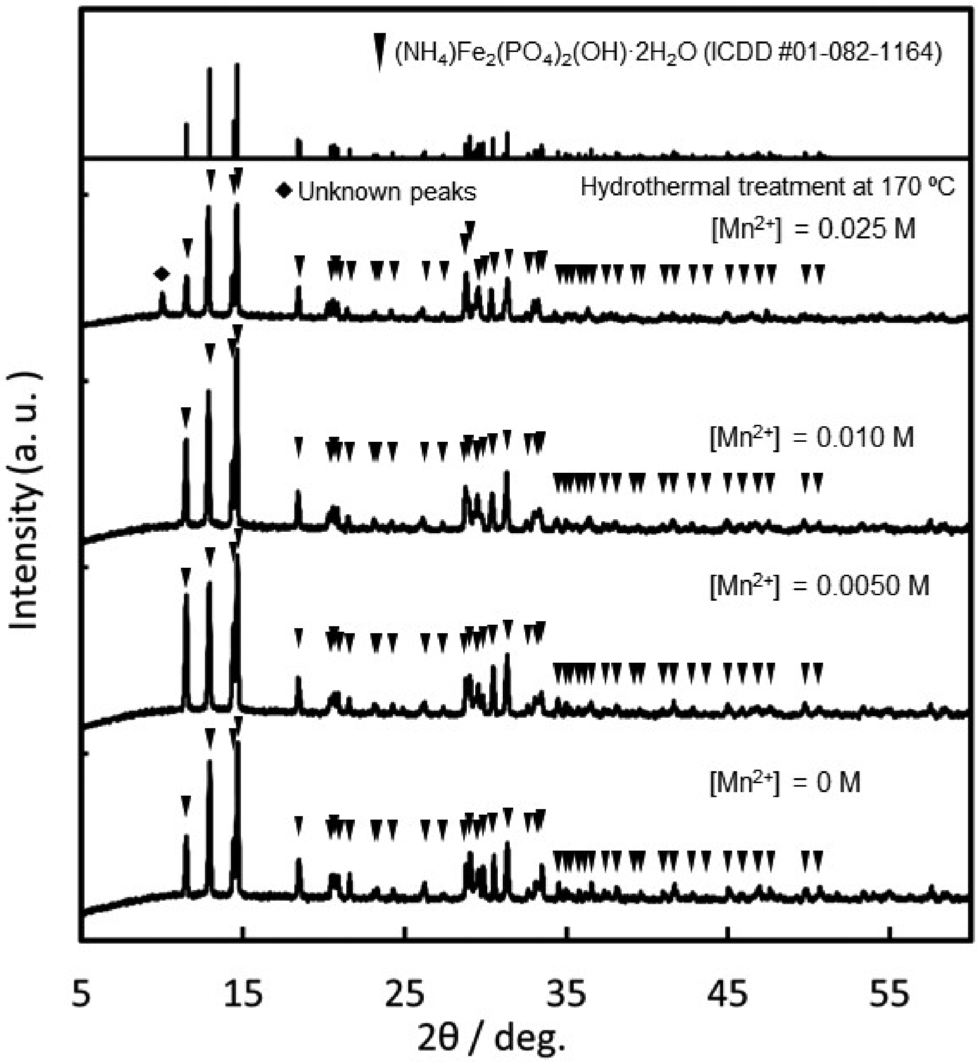

Fig. S6 XRD patterns of the Mn^{2+}-doped iron phosphate precipitates obtained at [$FeCl_3 \cdot 6H_2O$] = 0.10 M and [$MnCl_2 \cdot 4H_2O$] = 0–0.025 M by hydrothermal treatment at 170 °C.

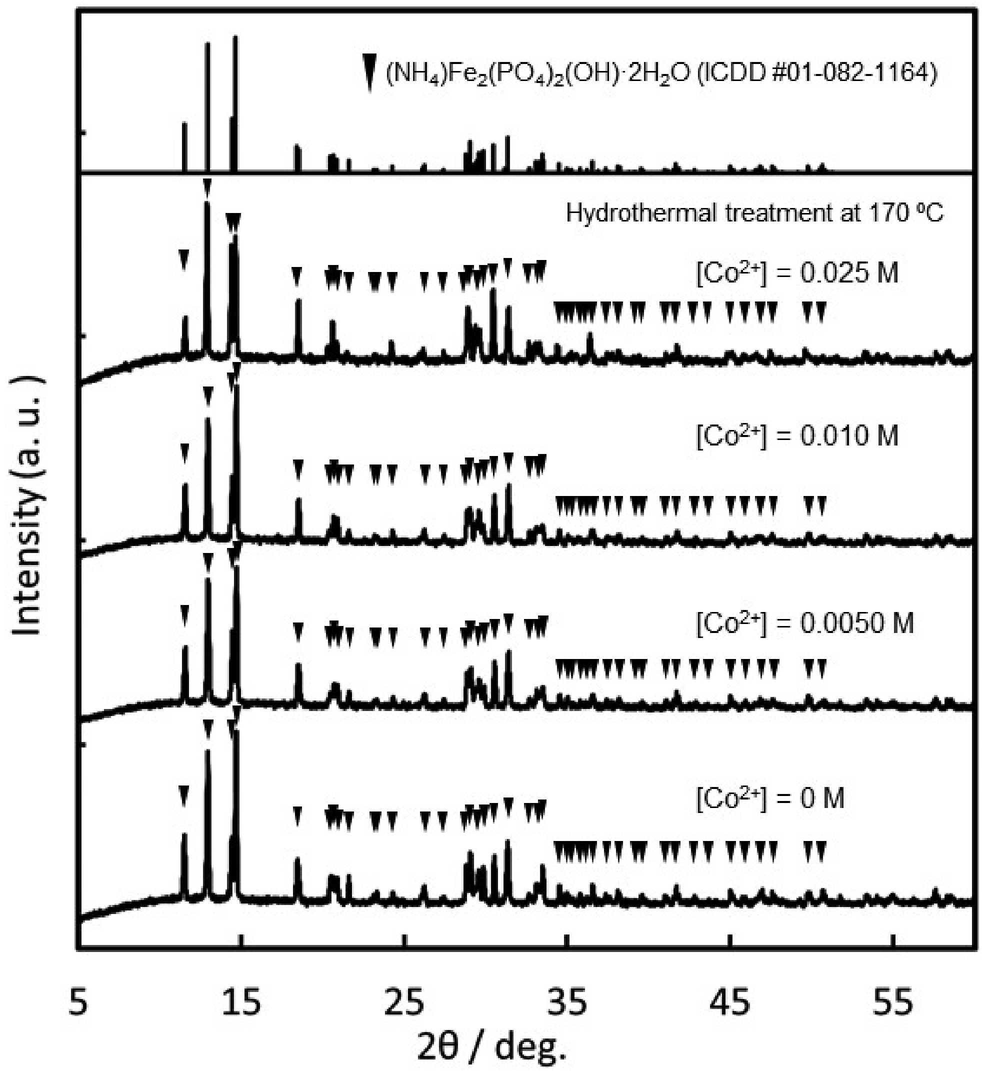

Fig. S7 XRD patterns of the Co^{2+}-doped iron phosphate precipitates obtained at [$FeCl_3 \cdot 6H_2O$] = 0.10 M and [$CoCl_2 \cdot 6H_2O$] = 0–0.025 M by hydrothermal treatment at 170 °C.

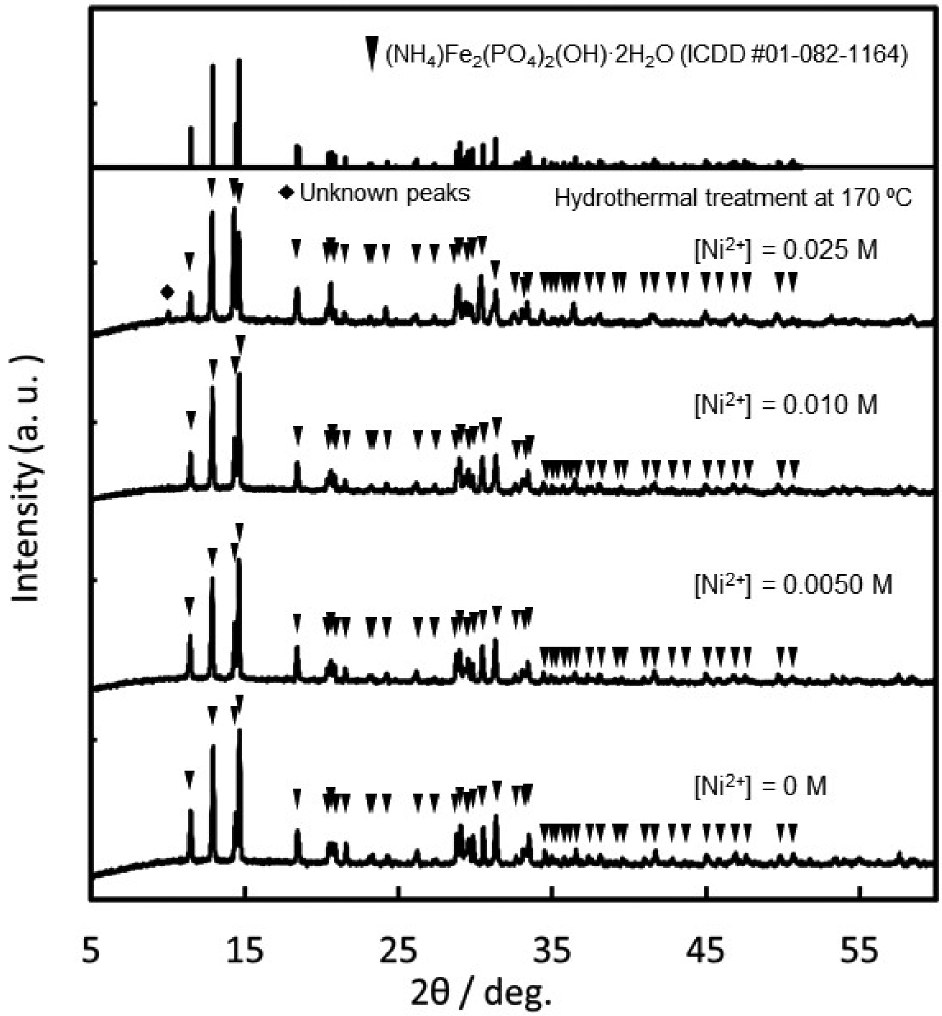

Fig. S8 XRD patterns of the Ni^{2+}-doped iron phosphate precipitates obtained at [$FeCl_3 \cdot 6H_2O$] = 0.10 M and [$NiCl_2 \cdot 6H_2O$] = 0–0.025 M by hydrothermal treatment at 170 °C.

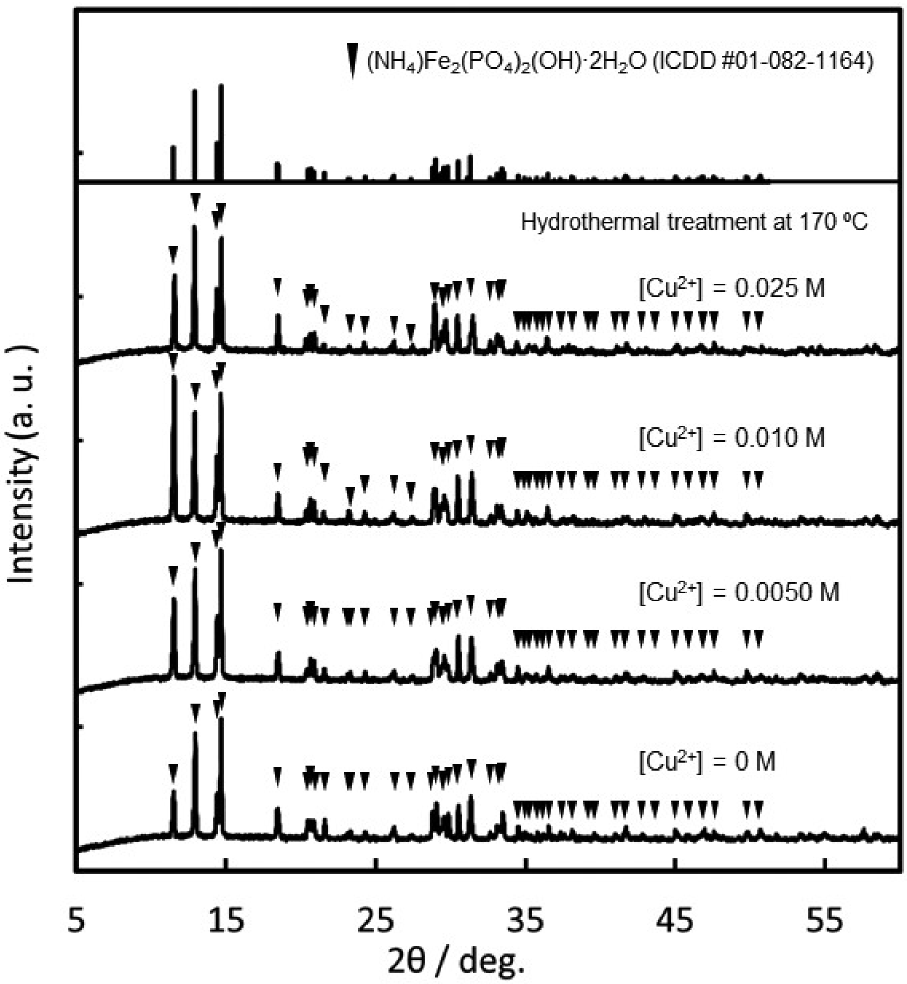

Fig. S9 XRD patterns of the Cu^{2+}-doped iron phosphate precipitates obtained at [$FeCl_3 \cdot 6H_2O$] = 0.10 M and [$CuCl_2$] = 0–0.025 M by hydrothermal treatment at 170 °C.

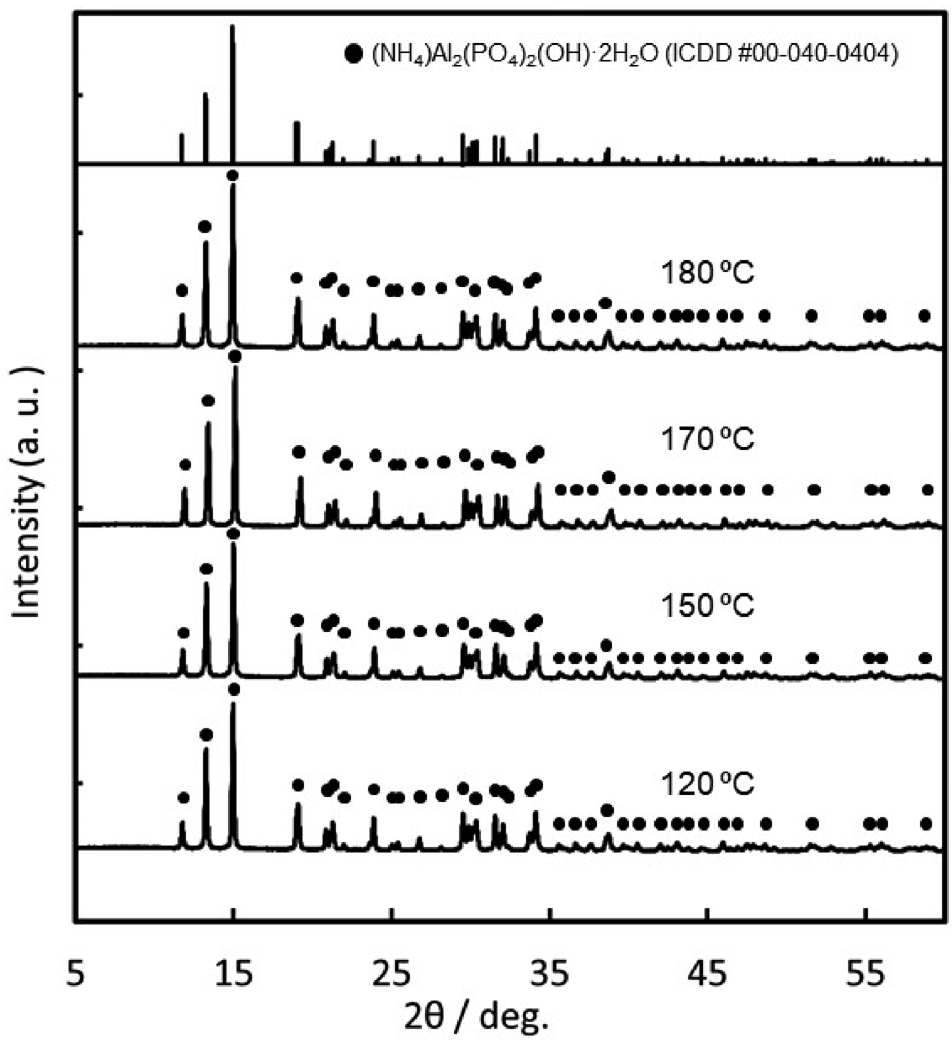

Fig. S10 XRD patterns of the ammoniotinsleyite samples obtained at [$AlCl_3$] = 0.10 M by hydrothermal treatment at 120–180 °C.

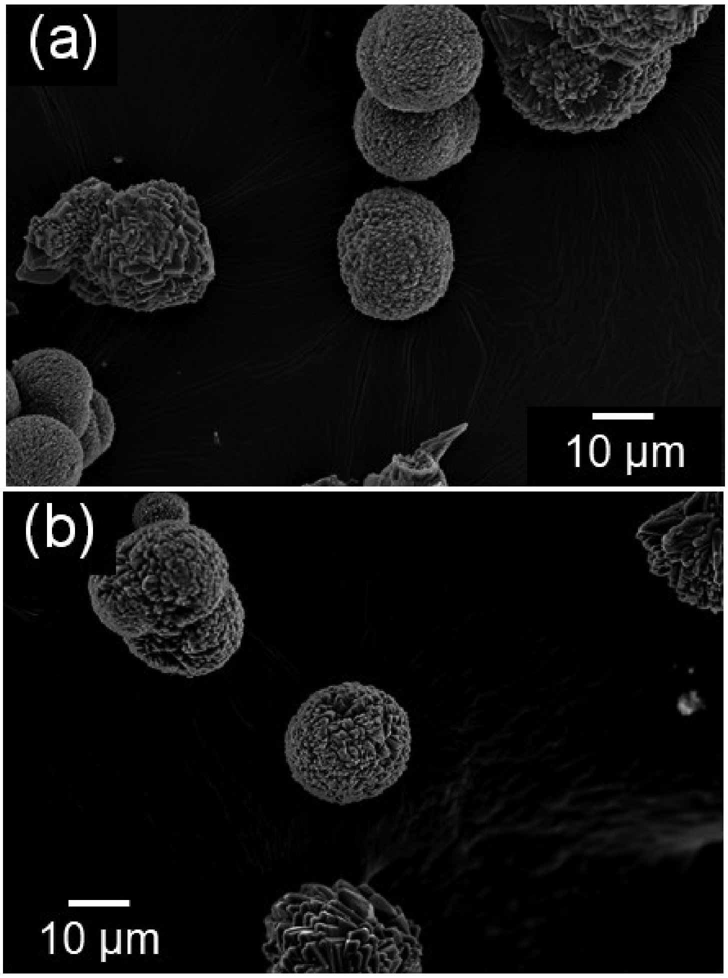

Fig. S11 SEM images of the ammoniotinsleyite samples obtained at [$AlCl_3$] = 0.10 M by hydrothermal treatment at 120 (a) and 170 (b) °C.

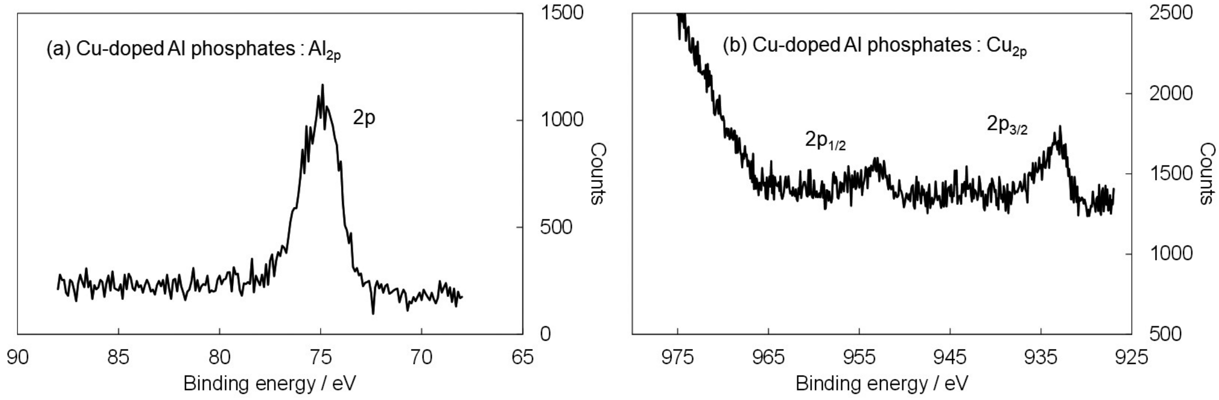

Fig. S12 XPS spectra of the Cu^{2+}-doped ammoniotinsleyite samples obtained at $[AlCl_3]$ = 0.10 M and $[CuCl_2]$ = 0.010 M by hydrothermal treatment at 170 °C; Al_{2p} (a) and Cu_{2p} (b).

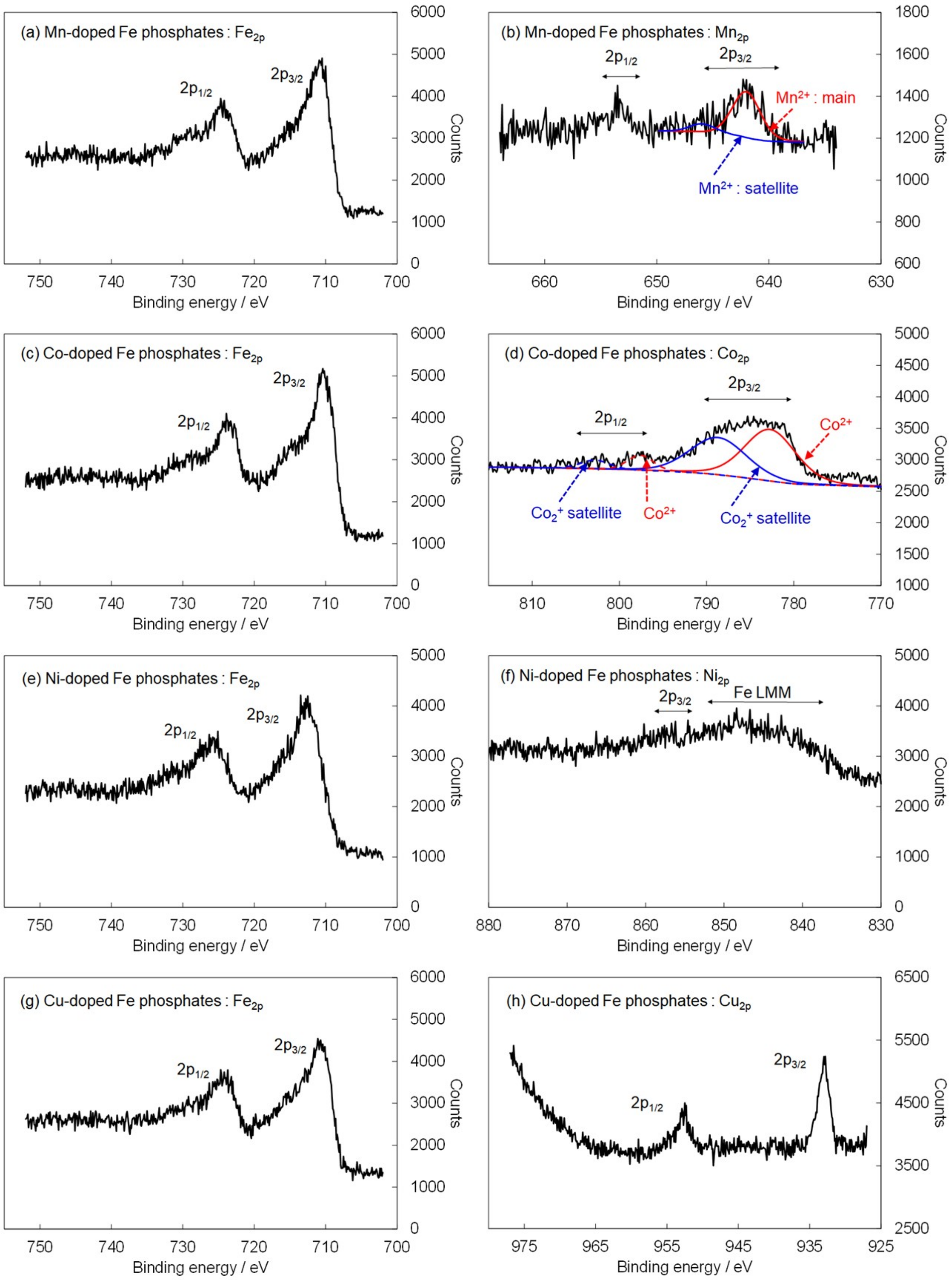

Fig. S13 XPS spectra of the transition metal-doped spheniscidite samples obtained at $[MnCl_2 \cdot 4H_2O]$ = 0.010 M, $[CoCl_2 \cdot 6H_2O]$ = 0.025 M, $[NiCl_2 \cdot 6H_2O]$ = 0.010 M or $[CuCl_2]$ = 0.025 M by hydrothermal treatment at 120 °C; Mn^{2+}-doped: Fe_{2p} (a) and Mn_{2p} (b), Co^{2+}-doped: Fe_{2p} (c) and Co_{2p} (d), Ni^{2+}-doped: Fe_{2p} (e) and Ni_{2p} (f), Cu^{2+}-doped: Fe_{2p} (g) and Cu_{2p} (h).